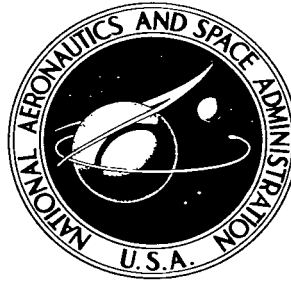


NASA TECHNICAL NOTE



NASA TN D-3649

NASA TN D-3649

c. 1



LOAN COPY: RETU  
AFWL (WLIL-  
KIRTLAND AFB, N

COMPARISON OF PANEL FLUTTER RESULTS  
FROM APPROXIMATE AERODYNAMIC THEORY  
WITH RESULTS FROM EXACT INVISCID  
THEORY AND EXPERIMENT

*by Sidney C. Dixon*  
*Langley Research Center*  
*Langley Station, Hampton, Va.*



TECH LIBRARY KAFB, NM



0130258

NASA TN D-3649

COMPARISON OF PANEL FLUTTER RESULTS FROM  
APPROXIMATE AERODYNAMIC THEORY WITH RESULTS FROM  
EXACT INVISCID THEORY AND EXPERIMENT

By Sidney C. Dixon

Langley Research Center  
Langley Station, Hampton, Va.

NATIONAL AERONAUTICS AND SPACE ADMINISTRATION

---

For sale by the Clearinghouse for Federal Scientific and Technical Information  
Springfield, Virginia 22151 - Price \$2.00

COMPARISON OF PANEL FLUTTER RESULTS FROM  
APPROXIMATE AERODYNAMIC THEORY WITH RESULTS FROM  
EXACT INVISCID THEORY AND EXPERIMENT

By Sidney C. Dixon  
Langley Research Center

SUMMARY

Flutter calculations for simply supported panels by means of both two-dimensional static (approximate) aerodynamic theory and linearized three-dimensional, unsteady, inviscid (exact) aerodynamic theory are presented and compared. The calculations indicate that for unstressed panels the results obtained from the approximate aerodynamic theory are in good agreement with the results obtained from the exact aerodynamic theory for Mach number  $M \geq 1.6$  and to even lower Mach numbers for length-width ratios  $2 \leq \frac{a}{b} \leq 6$ . For  $M < 1.6$  and  $\frac{a}{b} < 2$  the exact aerodynamic theory predicts single-degree-of-freedom instabilities which are not predicted by the approximate aerodynamic theory. These instabilities occur at a much lower value of dynamic pressure than is predicted by the approximate aerodynamic theory. The limited experimental results for the range of  $M \leq 1.6$  and  $a/b < 2$  indicate some decrease in the dynamic pressure required for flutter from that predicted by approximate aerodynamic theory, but by no means the decrease predicted by the exact aerodynamic theory. However, for the values of  $M$  and  $a/b$  where the two theories agree, there is also agreement with experiment. It is then shown that application of the exact aerodynamic theory does not remove the discrepancies that presently exist between theory and experiment for flutter of stressed panels. The inclusion of structural damping is found to have a large effect in some instances and can tend to eliminate some of the differences between theory and experiment for stressed panels. However, it is demonstrated that on the basis of small-deflection theory, damping has no effect on flutter of panels which are on the verge of buckling.

INTRODUCTION

Panel flutter is a self-excited oscillation of the external surface skin of a flight vehicle which results from the dynamic instability of the aerodynamic, inertia, and elastic forces of the system. The emergence of panel flutter as a significant design problem has motivated considerable experimental and theoretical research. These investigations have indicated the significance of such parameters as flow angularity (refs. 1 to 4), midplane

stress and buckling (refs. 5 to 7), cavity depth (refs. 8 to 10), initial imperfections (refs. 11 and 12), differential pressure (refs. 11 and 13), transverse shear stiffness (refs. 14 and 15), edge restraint (refs. 16 and 17), and orthotropic panel properties (refs. 3, 4, and 18). It should be noted, however, that most theoretical investigations have utilized two-dimensional static aerodynamic theory (both with and without damping) despite the fact that two-dimensional theory is considered applicable only for a limited range of panel length-width ratio and Mach number. The reason for extended use of this theory is that it greatly simplifies the problem and in some cases provides the only practical method of solution.

The present investigation was undertaken in an attempt to assess the useful range of the two-dimensional static aerodynamic theory approximation by means of an analysis that utilizes linearized three-dimensional potential flow theory for single finite panels. The latter analysis, which is by Cunningham (ref. 19), is used to determine the range of Mach number and length-width ratio for which the simpler aerodynamic approximation gives acceptable results. Results from these inviscid theories are obtained for both stressed and unstressed simply supported panels. The results for unstressed panels are compared with experimental results.

#### SYMBOLS

$$\bar{A} = \bar{R}_x - c_1 \left(\frac{a}{b}\right)^2$$

a panel length in x-direction

$$\bar{B} = \left(\frac{\omega}{\omega_r}\right)^2 + c_2 \bar{R}_y \left(\frac{a}{b}\right)^2 - c_3 \left(\frac{a}{b}\right)^4$$

b panel width in y-direction

$c_1, c_2, c_3$  constants dependent on cross-stream boundary conditions of panel

D flexural stiffness of panel,  $\frac{Eh^3}{12(1 - \nu^2)}$

E Young's modulus

g structural damping coefficient

h panel thickness

M Mach number

$M_n$	generalized mass of mode $n$
$m, n$	integers
$N_x$	inplane loading in x-direction (positive in compression)
$N_y$	inplane loading in y-direction (positive in compression)
$N_{x,cr}$	critical inplane load required for buckling
$Q_{nm}$	generalized aerodynamic force from the pressure due to mode $m$ and the modal deflection of mode $n$
$q$	dynamic pressure of airstream
$q_n$	time varying generalized coordinate of motion for mode $n$
$\bar{R}_x = \frac{N_x a^2}{\pi^2 D}$	
$\bar{R}_y = \frac{N_y a^2}{\pi^2 D}$	
$t$	time
$V$	velocity of airstream
$w$	lateral deflection of panel
$x, y$	Cartesian coordinates of panel
$\alpha, \delta, \epsilon$	parameters appearing in equations (2) and (3)
$\beta = \sqrt{M^2 - 1}$	
$\gamma$	mass density of panel
$\lambda = \frac{2qa^3}{\beta D}$	
$\frac{1}{\mu}$	mass density ratio, $\frac{\rho a}{\gamma h}$

- $\nu$             Poisson's ratio
- $\rho$             mass density of air
- $\omega$             flutter frequency
- $\omega_n$           natural frequency of mode  $n$
- $\omega_r$           reference frequency,  $\frac{\pi^2}{a^2} \sqrt{\frac{D}{\gamma h}}$

$$\nabla^4 = \frac{\partial^4}{\partial x^4} + \frac{2\partial^4}{\partial x^2 \partial y^2} + \frac{\partial^4}{\partial y^4}$$

### ANALYSIS

The results presented in this investigation were calculated by utilizing the analyses of Hedgepeth (ref. 20), Houbolt (ref. 21), Movchan (ref. 22), and Cunningham (ref. 19). The type of configuration considered is shown in figure 1. It consists of a single rectangular panel of uniform thickness  $h$  mounted in a rigid wall with air flowing over one surface at a Mach number  $M$ . The panel has a length  $a$  and a width  $b$  and is subjected to uniform midplane compressive forces  $N_x$  and  $N_y$  (considered positive in compression). The panel edges are either simply supported or clamped.

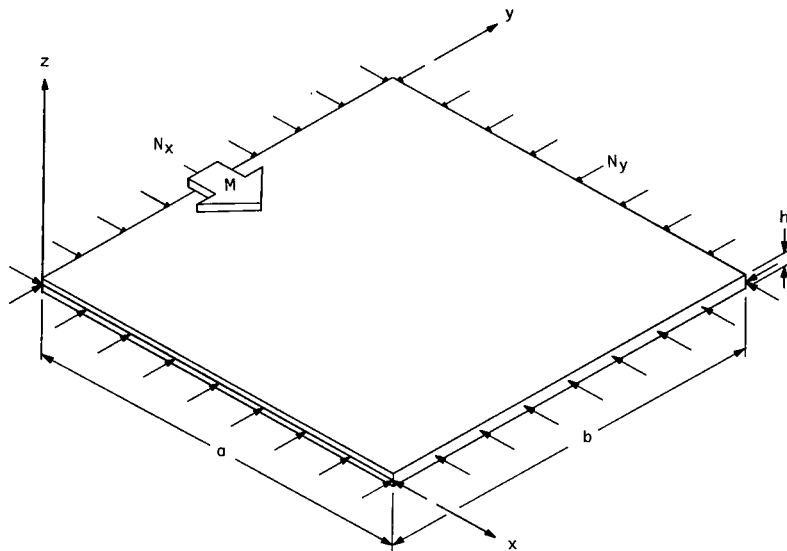


Figure 1.- Rectangular panel and coordinate system.

## Approximate Aerodynamic Theory

If the aerodynamic loading is represented by the two-dimensional static aerodynamic approximation, the governing partial differential equation is (ref. 20)

$$D\nabla^4 w + N_x \frac{\partial^2 w}{\partial x^2} + N_y \frac{\partial^2 w}{\partial y^2} + \gamma h \frac{\partial^2 w}{\partial t^2} + \frac{2q}{\beta} \frac{\partial w}{\partial x} = 0 \quad (1)$$

The closed-form solution to equation (1) has been obtained by Hedgepeth (ref. 20) for all edges simply supported and by Movchan (ref. 22) and Houbolt (ref. 21) for the leading and trailing edges simply supported or clamped, with the other two edges simply supported. In addition, Houbolt has obtained an approximate solution for all edges clamped. In his analysis, Houbolt assumed an approximate mode shape in the cross-stream direction in order to reduce the partial differential equation to an ordinary differential equation. The solution to the resulting ordinary differential equation, however, is exact. It should be noted that the aerodynamic loading term used by Houbolt and Movchan (if aerodynamic damping is neglected) differed from that used by Hedgepeth in that  $\beta$  was replaced by  $M$ . The use of the Ackeret value ( $\beta$ ) does not give significantly different results from the use of the "piston" theory ( $M$ ) except when  $M$  approaches 1.0.

The details of the solutions are in references 20 to 22 and only the appropriate stability equations necessary for solutions are presented herein.

When the leading and trailing edges are simply supported,

$$\left[ (\epsilon^2 + \delta^2)^2 + 4\alpha^2 (\delta^2 - \epsilon^2) \right] \sin \delta \sinh \epsilon = 8\alpha^2 \epsilon \delta (\cosh \epsilon \cos \delta - \cosh 2\alpha) \quad (2)$$

When the leading and trailing edges are clamped,

$$4\delta\epsilon (\cosh 2\alpha - \cosh \epsilon \cos \delta) = 2(-\epsilon^2 + \delta^2 + 4\alpha^2) \sinh \epsilon \sin \delta \quad (3)$$

where  $\alpha$ ,  $\delta$ , and  $\epsilon$  are related to  $\lambda$ ,  $\bar{A}$ , and  $\bar{B}$  by

$$\left. \begin{aligned} \delta^2 &= \frac{\lambda}{4\alpha} + \alpha^2 + \frac{\pi^2 \bar{A}}{2} \\ \epsilon^2 &= \frac{\lambda}{4\alpha} - \alpha^2 - \frac{\pi^2 \bar{A}}{2} \\ \bar{B} &= \frac{1}{\pi^4} \left[ \frac{\lambda^2}{16\alpha^2} - 4 \left( \alpha^2 + \frac{\pi^2 \bar{A}}{4} \right)^2 \right] \end{aligned} \right\} \quad (4)$$

The flutter parameter  $\lambda$ , the frequency parameter  $\bar{B}$ , and the length-width-ratio mid-plane load parameter  $\bar{A}$  are defined in the list of symbols. The constants in the parameters  $\bar{A}$  and  $\bar{B}$  depend on the boundary conditions at the side edges. Expressions for these constants for any value of rotational restraint are given in reference 17. For simply supported and clamped edges these parameters become (for a single half-wave in the y-direction):

For side edges simply supported,

$$\left. \begin{aligned} \bar{A} &= \bar{R}_x - 2\left(\frac{a}{b}\right)^2 \\ \bar{B} &= \left(\frac{\omega}{\omega_r}\right)^2 + \bar{R}_y\left(\frac{a}{b}\right)^2 - \left(\frac{a}{b}\right)^4 \end{aligned} \right\} \quad (5)$$

For side edges clamped,

$$\left. \begin{aligned} \bar{A} &= \bar{R}_x - 2.49\left(\frac{a}{b}\right)^2 \\ \bar{B} &= \left(\frac{\omega}{\omega_r}\right)^2 + 1.25\bar{R}_y\left(\frac{a}{b}\right)^2 - 5.14\left(\frac{a}{b}\right)^4 \end{aligned} \right\} \quad (6)$$

The expressions for  $\bar{A}$  and  $\bar{B}$  obtained by Houbolt (ref. 21) for clamped edges differ slightly from those given by equations (6) because he used  $\frac{1}{2}\left(1 - \cos \frac{2\pi y}{b}\right)$  for the assumed shape in the cross-stream direction, whereas the expressions in equation (6) were obtained from the fundamental clamped-clamped beam mode.

The eigenvalue  $\bar{B}$  can be computed for fixed values of  $\lambda$  and  $\bar{A}$  by varying  $\alpha$  until equations (2) and (3) are satisfied and then using the last of equations (4) to determine  $\bar{B}$ . The resulting solutions can be shown in the form of plots of  $\lambda$  as a function of  $\bar{B}$  for various values of  $\bar{A}$ . Such plots reveal that the critical value of  $\lambda$  (for no damping) occurs when the two lowest frequencies coalesce at the peak of the "frequency loop."

Movchan (ref. 22) noted that the stability equation (2) for simply supported panels is identically satisfied if

$$\left. \begin{aligned} \delta &= 2m\pi \\ \epsilon &= 2\alpha \\ m &= 1, 2, 3, \dots \end{aligned} \right\} \quad (7)$$

Substitution of equations (7) into the first two of equations (4) and solving for  $\lambda$  yields the following simple algebraic expression (for  $m = 1$ ):

$$\lambda = \frac{4}{3} \pi^3 \sqrt{\frac{4 - \bar{A}}{6}} (10 - \bar{A}) \quad (8)$$

Equation (8) has been referred to as the preflutter solution (ref. 22). The value of  $\lambda$  given by equation (8) falls on the frequency loop but below the peak; thus the term "preflutter." It is shown in reference 23 that equation (8) gives results in very close agreement with results obtained from equation (2) for unstressed panels for  $\frac{a}{b} > 1.0$ .

### Exact Aerodynamic Theory

Cunningham (ref. 19) has considered the flutter of a single finite panel on the basis of exact three-dimensional linearized supersonic potential flow (hereafter referred to as exact aerodynamics). The panel is considered to be finely divided into a large number of equal size boxes. The aerodynamic influence coefficient of each box on each other box is calculated and used in a modal-type flutter stability analysis. Because of the complexity of the problem, the analysis has been programed for solution on a digital computer.

The equation used by Cunningham in reference 19 to express the panel motion, which was derived from application of the Galerkin method, is

$$\left[ \omega^2 - \omega_n^2 (1 + ig) \right] M_n q_n + \sum_{m=1}^N Q_{nm} = 0 \quad (n = 1, 2, \dots, N) \quad (9)$$

The particular expressions for  $M_n$  and  $Q_{nm}$  are given in reference 19. It should be noted that equation (9) is valid only when there is no elastic or inertia coupling. In the present investigation equation (9) is used to obtain results only for simply supported panels, because for this case there is no elastic or inertia coupling and thus equation (9) is valid. The values of  $\omega_n^2$  used in equation (9) were obtained from the solution of equation (1) for no aerodynamic loading, which gives

$$\omega_n^2 = \omega_r^2 \left\{ \left[ n^2 + \left( \frac{a}{b} \right)^2 \right]^2 - \frac{n^2 N_x a^2}{\pi^2 D} - \frac{N_y a^2}{\pi^2 D} \left( \frac{a}{b} \right)^2 \right\} \quad (10)$$

where

$$\omega_r = \frac{\pi^2}{a^2} \sqrt{\frac{D}{\gamma h}}$$

As is usually the case with exact air forces, the flutter boundary cannot be computed directly, and an indirect method of computing and cross-plotting is required. The necessary procedure for obtaining flutter solutions and other pertinent details is thoroughly discussed in reference 19. It should be pointed out that, in addition to the structural damping coefficient  $g$  and reduced frequency  $\frac{\omega a}{V}$ , which appear in reference 19, other parameters necessary to obtain solutions based on the exact aerodynamic theory are the mass ratio  $\frac{1}{\mu}$  and the stiffness parameter  $\frac{\omega_1 a}{V}$ . These parameters are related to the flutter parameter  $\lambda$  appearing in the approximate aerodynamic theory by the relation (for simply supported edges)

$$\lambda = \frac{\pi^4 \left\{ \left[ 1 + \left( \frac{a}{b} \right)^2 \right]^2 - \frac{N_x a^2}{\pi^2 D} - \frac{N_y a^2}{\pi^2 D} \left( \frac{a}{b} \right)^2 \right\} \frac{1}{\mu}}{\left( \frac{\omega_1 a}{V} \right)^2 \beta} \quad (11)$$

## RESULTS AND DISCUSSION

### Unstressed Panels With Length-Width Ratios Greater Than 1.0

Comparison of theories.- Results for simply supported panels with  $\frac{a}{b} \geq 1.0$  are shown in figure 2 in terms of the flutter parameter  $\lambda^{1/3} \frac{b}{a}$  and length-width ratio  $\frac{a}{b}$ .

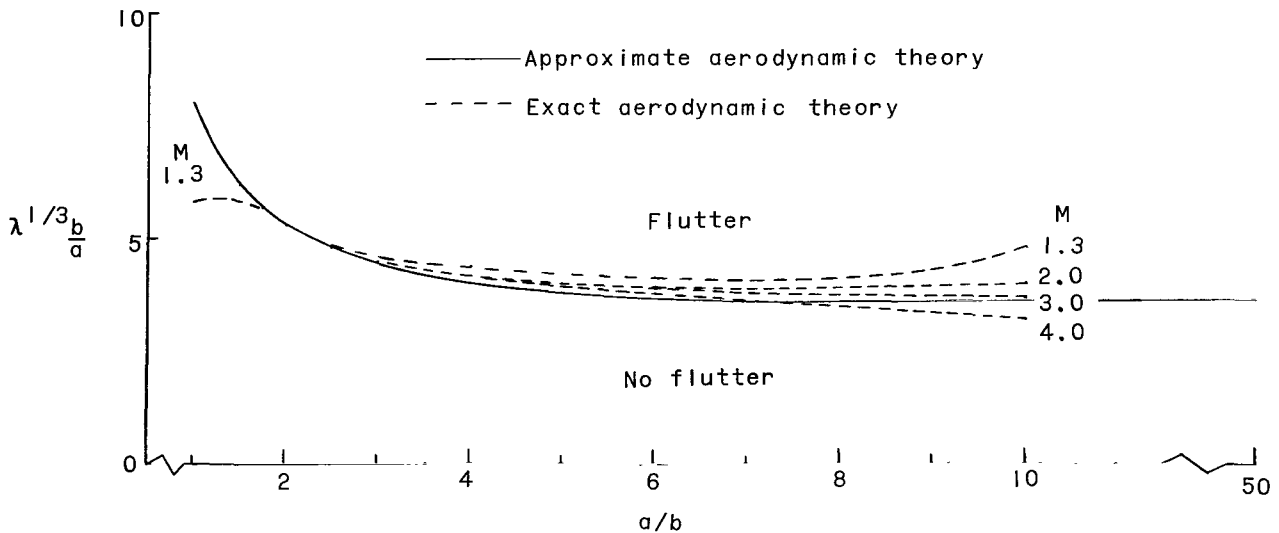


Figure 2.- Comparison of results obtained for flat unstressed simply supported panels with length-width ratios greater than 1.0.  $g = 0$ .

The solid curve was obtained from the closed-form solution (eq. (2)) based on the approximate aerodynamic theory. These results indicate that  $\lambda^{1/3} \frac{b}{a}$  decreases rapidly with increases in  $\frac{a}{b}$  up to approximately 2 or 3. The results also indicate that the dynamic pressure required for flutter is essentially independent of length for  $\frac{a}{b}$  greater than about 5 or 6.

The dashed curves shown in figure 2 represent flutter boundaries calculated by the use of Cunningham's analysis (ref. 19) utilizing exact aerodynamic theory for simply supported aluminum panels at sea level and for  $M$  of 1.3, 2, 3, and 4. All results for  $\frac{a}{b} \geq 4$  were obtained by using the first 12 natural modes of vibration (for a single half-wave in the  $y$ -direction) in the modal analysis; for  $\frac{a}{b} < 4$ , six modes were used. For these calculations the panels were divided into 400 boxes, 40 in the stream direction, and 10 in the cross-stream direction. The results based on exact aerodynamic theory nearly coincide with the results based on approximate aerodynamic theory for  $1 \leq \frac{a}{b} \leq 6$  and  $M$  from 2 to 4, and differ only slightly for  $2 \leq \frac{a}{b} \leq 6$  for  $M = 1.3$ . For  $M = 1.3$  and  $\frac{a}{b} < 2$  the exact aerodynamic theory indicates that the so-called single-degree-of-freedom instabilities are the critical flutter boundaries. This type of instability, which occurs in the low  $M$ , low  $\frac{a}{b}$  range, is discussed in more detail in the section entitled "Unstressed Panels With Length-Width Ratios Less Than 1.0."

For  $\frac{a}{b} > 6$  the differences between the two theories can be significant (although the agreement is still fair), depending on the Mach number. However, it is not certain that these differences are due only to aerodynamic effects as the modal solutions are not converged for  $\frac{a}{b}$  greater than about 6. The variation of  $\lambda^{1/3} \frac{b}{a}$  with the number of modes used in the analysis based on the exact aerodynamic theory is shown in figure 3 for  $\frac{a}{b} = 6$  and  $M = 1.3, 3, \text{ and } 4$ . Convergence of a Galerkin solution is determined by using more and more modes in the analysis until additional modes do not alter the flutter boundary significantly. The results shown in figure 3 suggest that the critical mode 2-1 boundaries are not fully converged when 12 modes are used. (In this discussion, the flutter boundaries obtained from the exact aerodynamic theory are described by reference to the two most predominant vibration modes in the flutter mode shape.) In addition, the rate of convergence does not appear to be significantly affected by variations in Mach number. The number of modes required for convergence of flutter solutions based on the Galerkin method and approximate aerodynamic theory was investigated in reference 4. This investigation revealed that 12 modes were sufficient for convergence for a simply supported panel with  $\frac{a}{b} = 5$ , but that 60 modes were required when  $\frac{a}{b}$  was increased to 10. For  $\frac{a}{b}$  of 10, 12 modes gave values of  $\lambda^{1/3} \frac{b}{a}$  of approximately 80 percent of the

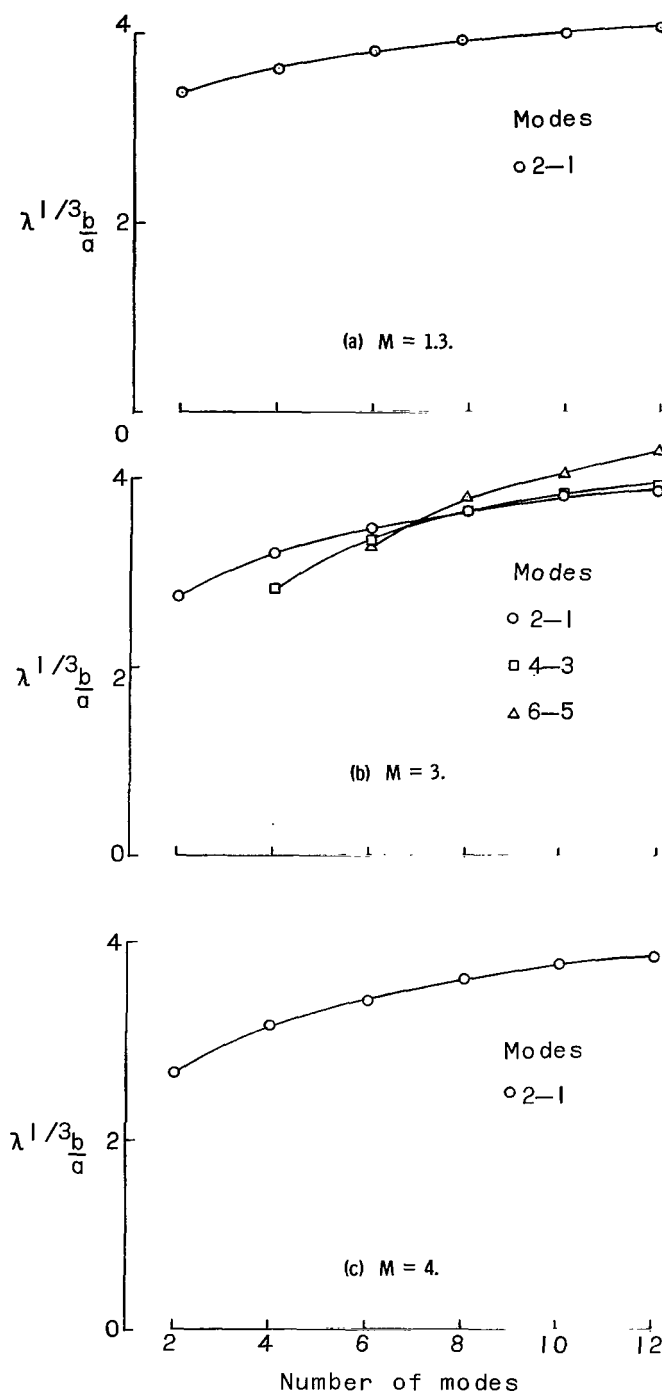


Figure 3.- Variation of  $\lambda^{1/3} \frac{b}{a}$  with number of modes used in analysis.  $\frac{a}{b} = 6$ .

converged value. Thus, the results shown in figure 2 for  $\frac{a}{b}$  greater than about 6 must be considered approximate because of nonconvergence of the modal solutions. For  $2 \leq \frac{a}{b} \leq 6$  the critical boundary always corresponded to a mode 2-1 boundary, as was the case for all values of  $\frac{a}{b}$  for the approximate aerodynamic theory. For  $\frac{a}{b} > 6$  the exact aerodynamic theory indicated that higher mode boundaries could become the critical boundaries; this result is attributed to nonconvergence of the solution. For example, figure 3(b) shows that the mode 4-3 or 6-5 boundaries were the critical boundaries for  $\frac{a}{b} = 6$  when less than 8 modes were used but the mode 2-1 boundary became the critical boundary when more than 8 modes were used. For this reason it is assumed that if convergence could have been obtained at the higher values of  $\frac{a}{b}$  the flutter boundary would correspond to the mode 2-1 boundary. Thus the results shown in figure 2 for  $\frac{a}{b} > 6$  are the mode 2-1 results.

The results obtained from the exact aerodynamic theory were essentially independent of variations in material and altitude, or mass density ratio. For example, figure 4 shows the variation of  $\lambda^{1/3} \frac{b}{a}$  with  $\frac{1}{\mu}$  for  $\frac{a}{b} = 4$  and  $M = 3$ . The solid curve represents the mode 2-1 boundary obtained from a 6-mode solution; the circle at  $\frac{1}{\mu} = 0$  indicates the value of

$\lambda^{1/3} \frac{b}{a}$  obtained from the approximate aerodynamic theory. As can be seen from the figure,  $\lambda^{1/3} \frac{b}{a}$  varies only slightly with  $\frac{1}{\mu}$ . The intersection of the dashed line with the flutter boundary is the flutter point for an aluminum panel at sea level. For denser materials or higher altitudes the flutter point would be to the left of the one shown, but the critical value of  $\lambda^{1/3} \frac{b}{a}$  would change only slightly. Hence,  $\lambda^{1/3} \frac{b}{a}$  is essentially independent of variation in material and altitude. Such behavior is typical of all the converged results

obtained for  $\frac{a}{b} \geq 1$  except for  $\frac{a}{b} < 2$  and  $M = 1.3$ . Thus the mode 2-1 flutter boundary is essentially described by the single parameter  $\lambda$  which combines the independent variables  $\omega_1 \frac{a}{V}$  and  $\frac{1}{\mu}$  (see

eq. (11)) given by the exact aerodynamic theory. Moreover, the calculations reveal that the critical values of  $\lambda^{1/3} \frac{b}{a}$  were essentially independent of structural damping (up to  $g = 0.025$ ) except for  $\frac{a}{b} < 2$  and  $M = 1.3$ . The good agreement of the results obtained from the approximate aerodynamic theory with the results of the exact theory, and the virtual independence of the flutter parameter  $\lambda^{1/3} \frac{b}{a}$  on variations in material, altitude, and damping, suggest that the approximate aerodynamics is useful for theoretical investigations of the various factors affecting panel flutter. References 9 and 10 present flutter results obtained from both the approximate and exact aerodynamic theories for clamped panels from which the same conclusion can be drawn.

**Comparison of theory and experiment.** - A comparison of experiment with theoretical results based on the approximate aerodynamic theory for  $\frac{a}{b} \geq 1$  in terms of the flutter parameter  $\lambda^{1/3} \frac{b}{a}$  and  $\frac{a}{b}$  is shown in figure 5. The solid curve is for simply supported panels (eq. (2)) and the dashed curve is for clamped panels (eq. (3)). The circles represent published (refs. 5, 13, and 24 to 28) and unpublished experimental flutter points obtained at a Mach number of 3.0 for essentially flat panels tested under aerodynamic heating conditions. These data are for edge restraints between simply supported and clamped conditions and were obtained from tests that involved thermal midplane stresses.

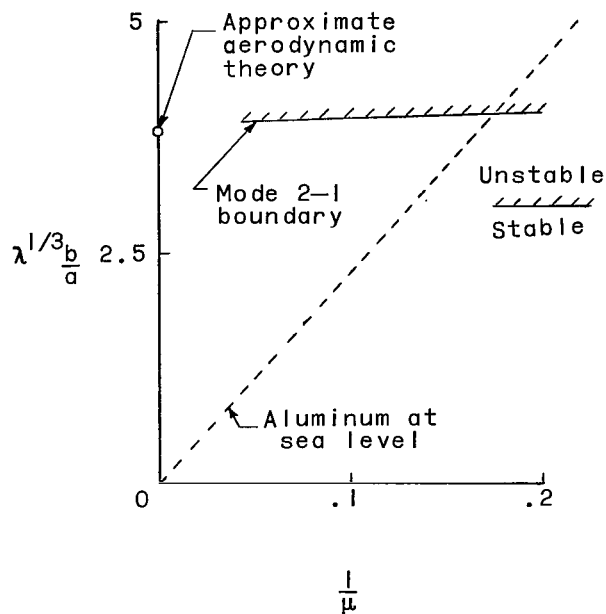


Figure 4.- Variation of  $\lambda^{1/3} \frac{b}{a}$  with  $1/\mu$  typical of cases where results from exact and approximate aerodynamic theories agree.  $M = 3$ ;  $\frac{a}{b} = 4$ ;  $g = 0$ .

However, data were obtained sufficiently close to zero thermal stress that an extrapolation could be made to get essentially zero stress flutter points. The other symbols shown in figure 5 represent flutter points for essentially clamped panels (ref. 9) obtained at various Mach numbers from 1.2 to 5. The scatter in the data shown is due in part to difficulties in extrapolating to zero stress points (for  $M = 3.0$ ), variations in panel supports, and variations in Mach number. It should be pointed out that the large variation of the flutter parameter for the experiments at  $\frac{a}{b}$  of 1.37 and 2.18 did not appear to be primarily associated with Mach number as the variation was of a random nature. (See

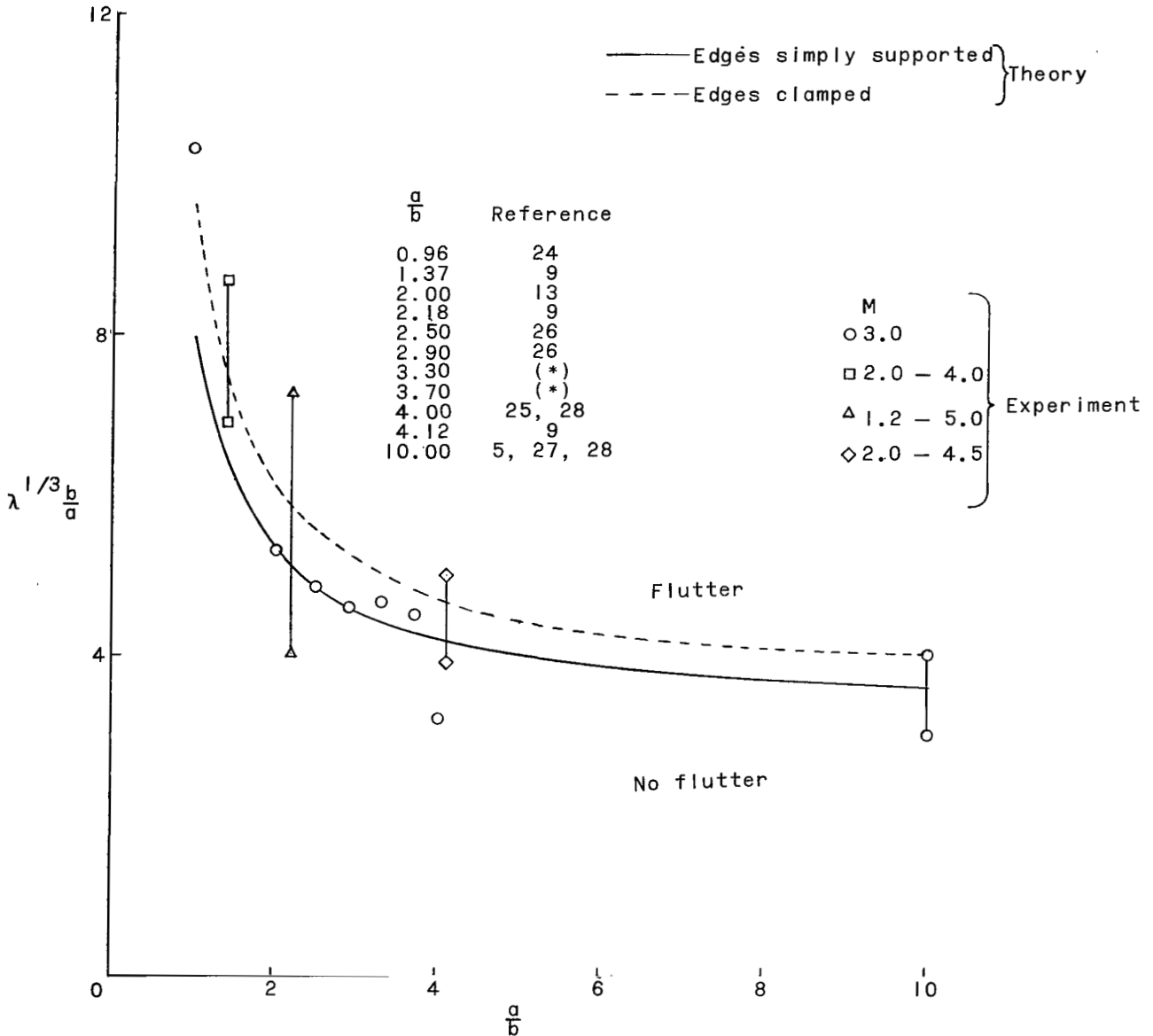


Figure 5.- Comparison of experiment with approximate aerodynamic theory for  $\frac{a}{b} \geq 1.0$ .  $N_x = N_y = 0$ .  
 \*Previously unpublished results obtained from investigation similar to the one described in reference 26.

ref. 9.) Such scatter is fairly typical of panel flutter experiments when data are obtained from a variety of configurations. The scatter in the data at  $\frac{a}{b}$  of 2.18, 4, and 10 indicates that the theory can give unconservative predictions of the value of  $\lambda^{1/3} \frac{b}{a}$  required for flutter by as much as 25 percent. However, when the entire range of  $\frac{a}{b}$  from 1 to 10 is considered, the agreement between theory and experiment appears to be reasonable. It should be noted that the flutter points at  $\frac{a}{b}$  of 10 were obtained from arrays of panels. In addition, one of the flutter points at  $\frac{a}{b}$  of 10 was obtained from wind-tunnel tests of a full-size component of an existing vehicle (ref. 28). Thus, the flutter of an array of panels (4 bays in cross-stream direction) was adequately predicted by theoretical results for a single panel.

### Unstressed Panels With Length-Width Ratios Less Than 1.0

Comparison of theories.- Results obtained from both the exact and approximate aerodynamic theories for  $\frac{a}{b} \leq 1.0$  are shown in figure 6 in terms of the flutter parameter  $\lambda^{1/3}$  and the panel length-width ratio  $\frac{a}{b}$ . The solid curve was obtained from the approximate aerodynamic theory. The approximate aerodynamic theory predicts that the parameter  $\lambda^{1/3}$  decreases rapidly as  $\frac{a}{b}$  decreases from 1 to 0.75 but decreases only slightly for  $\frac{a}{b} < 0.75$ . The dashed curves were obtained from the exact aerodynamic theory by using 6 modes for aluminum panels at sea level for  $M = 1.3, 1.5, 1.6, 2,$  and  $3$ .

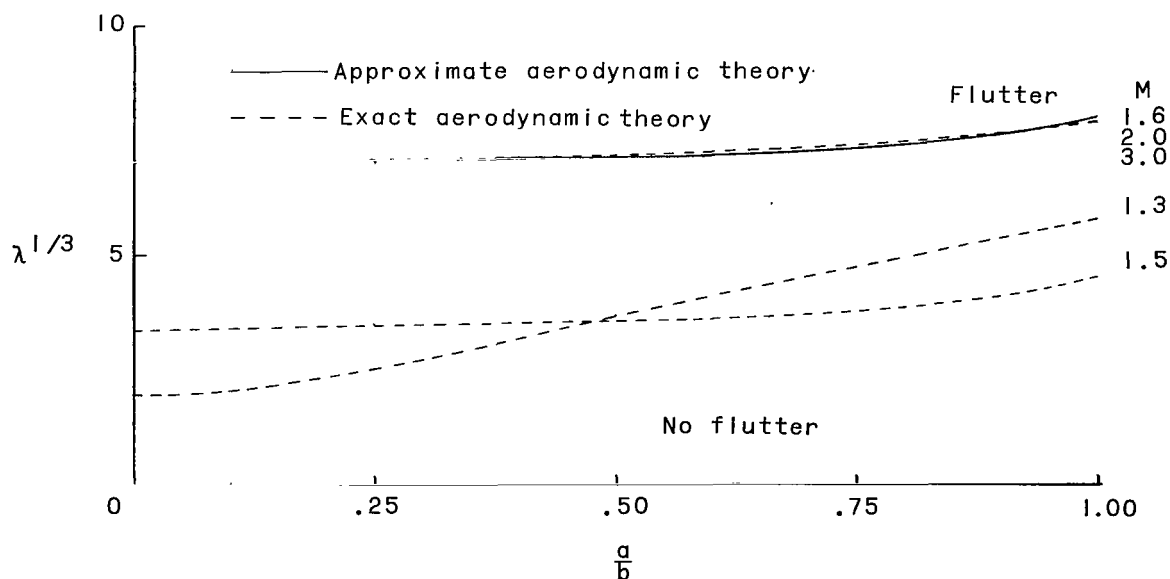


Figure 6.- Comparison of results obtained from exact and approximate aerodynamic theories for flat unstressed simply supported aluminum panels with length-width ratios less than 1.0.  $g = 0$ ; sea level.

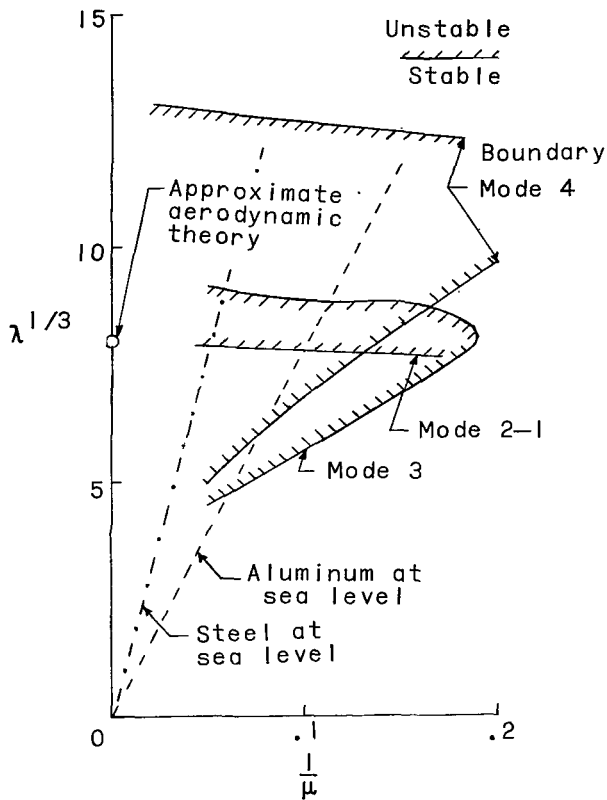


Figure 7.- Variation of  $\lambda^{1/3}$  with the mass-ratio parameter  $1/\mu$ . All results obtained from 6 mode analysis.  $M = 1.4$ ;  $\frac{a}{b} = 1.0$ ;  $g = 0$ .

figure 7, the single-degree-of-freedom boundaries are double valued and indicate large variations of  $\lambda^{1/3}$  with  $\frac{1}{\mu}$ . Calculations indicate that the unstable regions shrink with increasing structural damping coefficient  $g$  and may vanish sometimes for extremely small values of  $g$ . It is interesting to note that the mode 2-1 boundary is essentially independent of  $\frac{1}{\mu}$  (and also of  $g$ ) and is very close to the value of  $\lambda^{1/3}$  given by the approximate aerodynamic theory. More detailed discussions of single-degree-of-freedom instabilities are presented in references 9, 19, 29, and 30.

The single-degree-of-freedom instabilities gave the critical boundaries in all cases for  $M \leq 1.5$ . As can be seen from figure 6, the results obtained from the exact aerodynamic theory indicate large decreases in  $\lambda^{1/3}$  as  $M$  is decreased below 1.6. This decrease has been attributed in part to the change in flutter mechanism and to "negative" aerodynamic damping (see, for example, ref. 9). The results shown in figure 6 are for aluminum panels at sea level and for  $g = 0$ . For other altitudes, materials, and values of structural damping coefficient  $g$ , the results could be expected to be significantly different. Other investigations (refs. 30 and 31) have indicated that for  $M < 1.5$  flutter

The results obtained from the exact aerodynamic theory for  $M \geq 1.6$  show the same trend as the results obtained from the approximate aerodynamic theory and are in excellent numerical agreement; the critical boundaries were the mode 2-1 boundaries. For  $M < 1.6$  the exact aerodynamic theory predicts the so-called single-degree-of-freedom instabilities that are not predicted by the approximate aerodynamic theory.

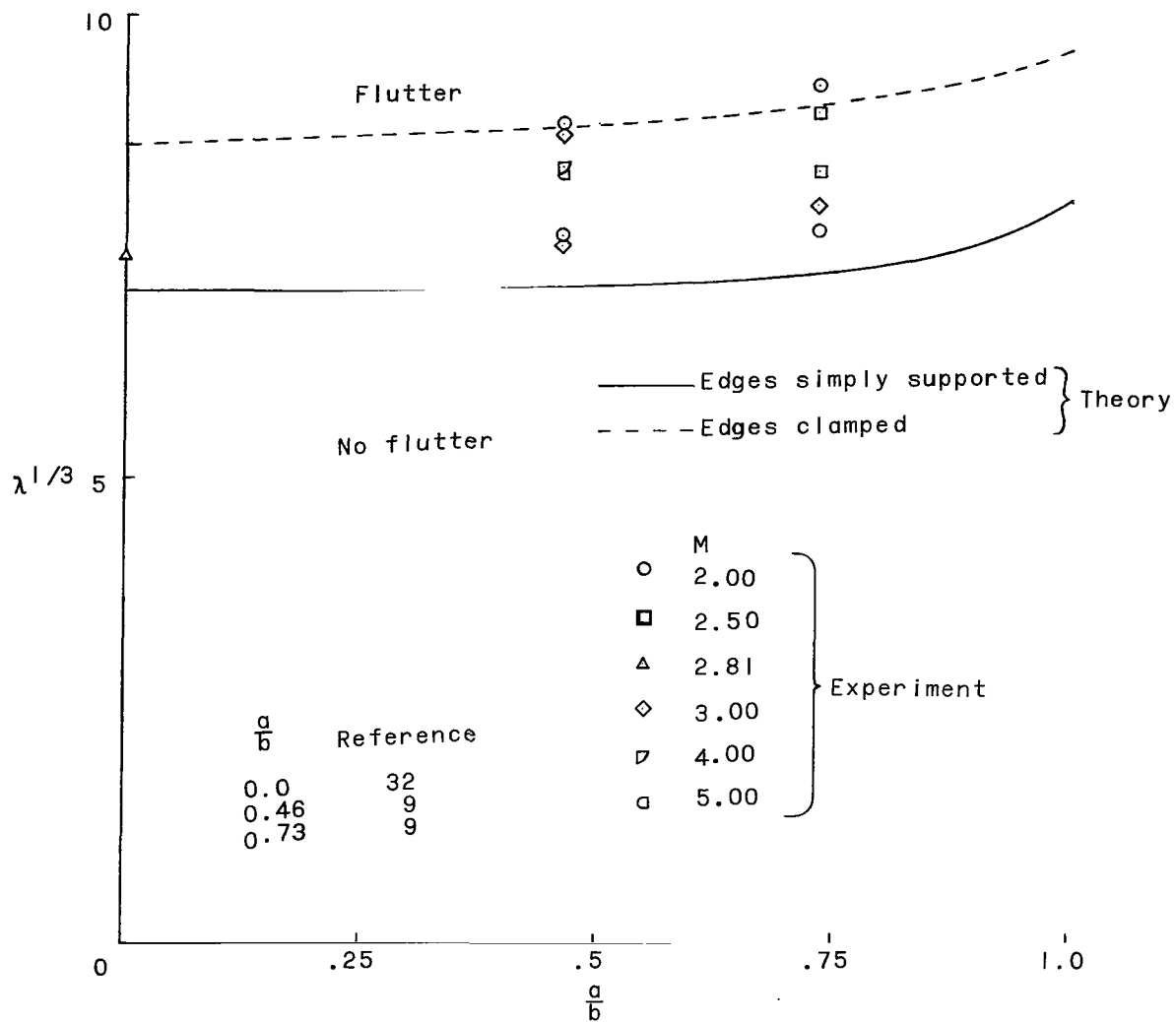
The single-degree-of-freedom instabilities are characterized by the fact that the flutter mode shape and frequency essentially correspond to one of the natural modes of the panel. Typical single-degree-of-freedom flutter boundaries are shown in figure 7 in terms of the flutter parameter  $\lambda^{1/3}$  and the mass density ratio parameter  $\frac{1}{\mu}$ . The results are for  $\frac{a}{b} = 1.0$ ,  $M = 1.4$ . Three flutter boundaries are shown, the coupled mode 2-1 boundary, and the mode 3 and mode 4 single-degree-of-freedom boundaries. As can be seen from

boundaries are sensitive to boundary-layer effects and the validity of the inviscid theory thus may be questioned. Because of the sensitivity of the flutter boundaries to such factors as variations in material and structural damping, the boundaries shown in figure 6 are probably not useful for design purposes for  $M < 1.6$ . They are presented solely to indicate the large variations of  $\lambda^{1/3}$  with  $M$  as indicated by the exact aerodynamic theory for  $\frac{a}{b} < 1$  and  $M \leq 1.5$ .

Calculations were also made by using three-dimensional static aerodynamic theory in order to investigate the three-dimensional effects alone (that is, unsteady effects neglected). The results were obtained from the flutter determinant of Hedgepeth (ref. 20) by using four terms in the stream direction and two terms in the cross-stream direction. Calculations were made for  $M = 1.4$ ,  $\frac{a}{b} = 0.245$  and for  $M = 1.3$ ,  $\frac{a}{b} = 0.208$ . Both cases correspond to values of  $\beta \frac{b}{a} = 4.0$ . The calculations revealed that the critical flutter boundary was the coupled mode 2-1 boundary, that no single-degree-of-freedom instabilities existed, and that the critical values of  $\lambda^{1/3}$  were very close to the values obtained from the two-dimensional static aerodynamic theory. Thus, for  $\frac{a}{b} < 1$  three-dimensional effects appear to be insignificant and the unsteady effect appears to be the significant factor, as might have been expected from the results of previous investigations. (See, for example, ref. 20.)

Comparison of theory and experiment. - A comparison of experimental results for  $M \geq 2$  with theoretical results based on the approximate aerodynamic theory for  $\frac{a}{b} < 1.0$  in terms of the flutter parameter  $\lambda^{1/3}$  and  $\frac{a}{b}$  is shown in figure 8(a). The solid curve is for simply supported panels (eq. (2)) and the dashed curve is for clamped panels (eq. (3)). The experimental results for  $\frac{a}{b}$  of 0.46 and 0.73 are for panels essentially clamped on all edges (ref. 9). The result for  $\frac{a}{b} = 0$  was obtained from a panel clamped on the leading edge, simply supported on the trailing edge, and free on the side edges (ref. 32). Such a panel would behave essentially like a beam and this two-dimensional behavior is assumed representative of semi-infinite panels ( $\frac{a}{b} = 0$ ). As can be seen from figure 8(a), the agreement between theory and experiment is good for the entire range of  $\frac{a}{b}$  shown; the boundary for simply supported edges gives a lower bound for the experimental data.

A comparison of experimental results with theoretical results for  $M < 2$  and  $\frac{a}{b} < 1.0$  is shown in figure 8(b). The symbols represent experimental flutter points obtained from panels with various edge restraints at various Mach numbers from 1.1 to 1.6 (refs. 9, 33, 34, and 35). The results for  $\frac{a}{b} = 0$  were obtained from panels with free side edges. As can be seen from figure 8(b), the theory based on the approximate aerodynamics is in only fair to good agreement with experiment for  $\frac{a}{b} < 1$  and  $M < 1.6$  as

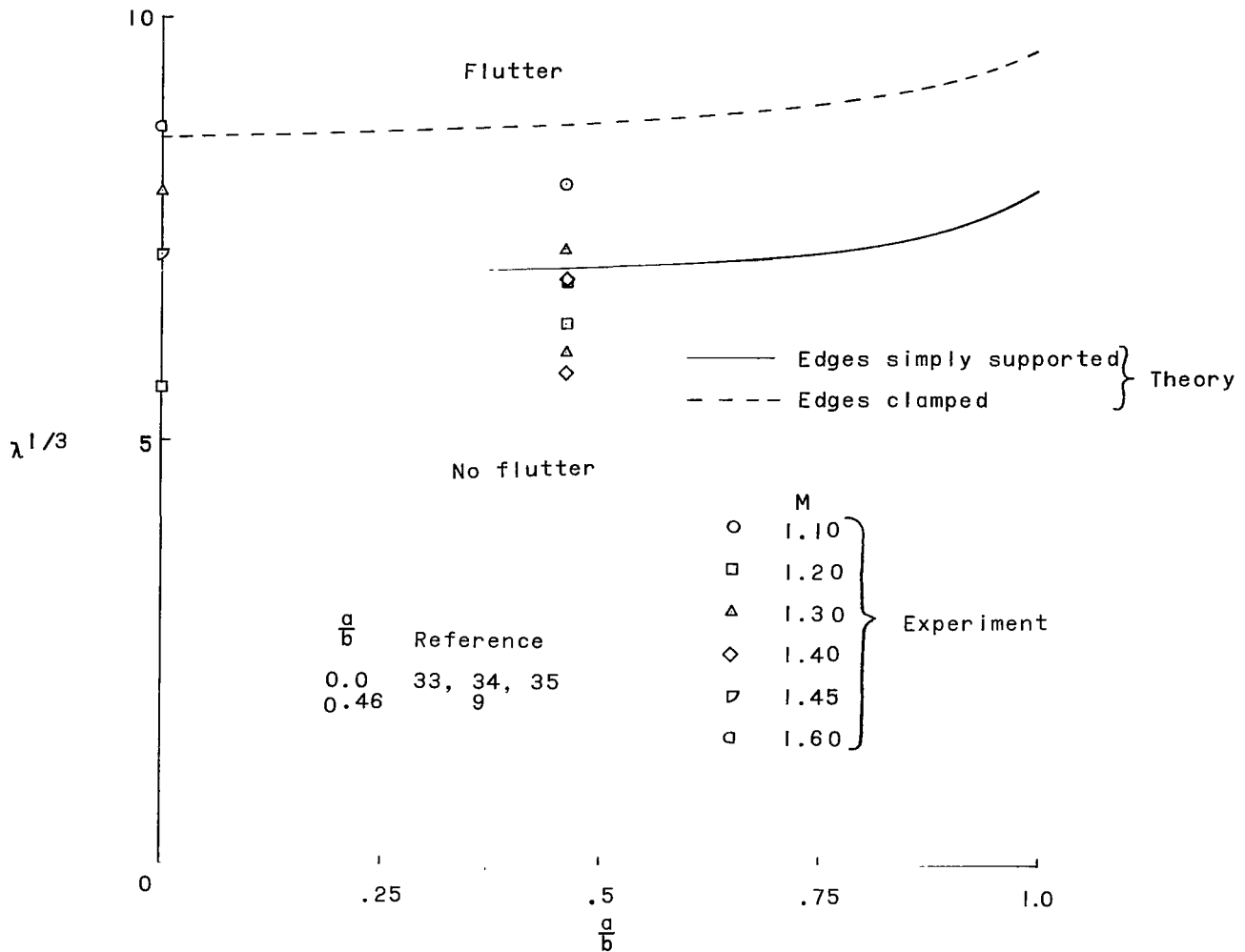


(a)  $M \geq 2.0$ .

Figure 8.- Comparison of experiment with approximate aerodynamic theory for  $\frac{a}{b} < 1.0$ .

the experimental data are not bounded by the theoretical boundaries. The data indicate the theory can give unconservative predictions of the value of  $\lambda^{1/3}$  required for flutter by as much as 20 percent.

The experimental results are not compared with theoretical results obtained from the exact aerodynamic theory for  $\frac{a}{b} < 1$  and  $M < 1.6$  because the theoretical results are very sensitive to variations in structural damping coefficient  $g$ . However, such comparisons have been made in other investigations (for example, refs. 9, 19, and 33). These comparisons have revealed that for no structural damping ( $g = 0$ ) the results are in poor quantitative and qualitative agreement with experiment. The inclusion of structural damping tends to improve the agreement. However, the boundaries obtained from the



(b)  $M < 2.0$ .

Figure 8.- Concluded.

exact aerodynamic theory are extremely sensitive to structural damping and the appropriate value of  $g$  to use for calculations generally is not known. Thus the usefulness of the exact aerodynamic theory, as presently employed, for predicting flutter for the low range of  $\frac{a}{b}$  and  $M$  may be limited.

The discrepancies that now exist between experiment and exact aerodynamic theory have been attributed to several factors such as transonic nonlinearities (ref. 9) and boundary layer (ref. 33). In addition, Dowell and Voss (ref. 9) have suggested that another possibility for the discrepancies between theory and experiment is that the theoretical flutter solution is incomplete. That is, at present only neutral stability boundaries have been computed. It is possible that the complete solution would indicate that the most

critical boundaries calculated from the exact aerodynamic theory for low  $M$  and low  $\frac{a}{b}$  would prove to be very weak instabilities and, perhaps, insignificant.

### Stressed Panels

For stressed isotropic panels, experimental data indicate that the most critical portion of the flutter boundary occurs at the transition from the flat unbuckled boundary to the postbuckled boundary (for example, ref. 5). However, theoretical results based on the approximate aerodynamic theory indicate that the most critical condition can occur at values of midplane load considerably less than that required for buckling (refs. 6, 36, and 37). It has been suggested that the discrepancies between theoretical and experimental results for stressed panels are due in part to the use of static aerodynamics (ref. 36). Thus, some results are considered for stressed panels based on exact aerodynamic theory which, of course, includes the unsteady effects.

Comparison of theories for long panel ( $\frac{a}{b} = 4.0$ ).- Theoretical results for a simply supported panel obtained from both the two-dimensional static and exact aerodynamic theories are shown in figure 9. The results obtained from exact aerodynamic theory were calculated from a 6 mode solution for aluminum panels at sea level for  $M = 3.0$ ;

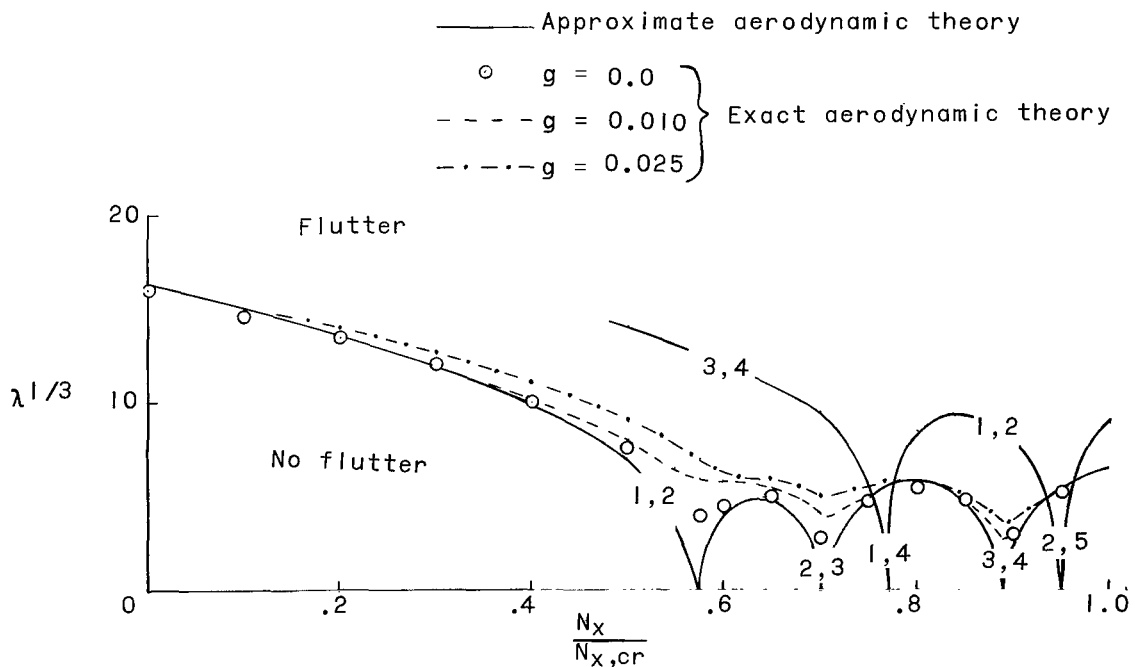


Figure 9.- Comparison of results obtained from exact and approximate aerodynamic theories for flat simply supported panel subjected to midplane compressive load.  $M = 3.0$ ;  $\frac{a}{b} = 4.0$ ;  $\frac{N_y}{N_x} = 0$ . The numbers on the curves indicate the modes that coalesced for flutter.

this value of  $M$  corresponds to the value at which most published experimental data for stressed panels have been obtained. The results are presented in terms of the flutter parameter  $\lambda^{1/3}$  and  $\frac{N_x}{N_{x,cr}}$ , the ratio of the midplane compressive load to the critical value required for buckling for no airflow. The solid curves represent the two lowest flutter boundaries obtained from the approximate aerodynamic theory; the numbers on the curves indicate the modes that coalesced for flutter. As can be seen from figure 9, one boundary obtained from the approximate aerodynamic theory indicates that zero values of the flutter parameter occur at values of  $\frac{N_x}{N_{x,cr}}$  of approximately 0.58, 0.71, and 0.89, and also that the flutter mode changes from a combination of modes 1 and 2 to a combination of modes 3 and 4. The other boundary, which corresponds to a higher mode boundary at the lower values of stress ratio, also indicates zero values of  $\lambda^{1/3}$  and variation in flutter mode as the stress is increased.

The circles in figure 9 represent flutter points obtained from exact aerodynamic theory for no structural damping. As can be seen, these results are in excellent quantitative agreement with the results based on the approximate aerodynamic theory except near the critical values of  $\frac{N_x}{N_{x,cr}}$  where the aerodynamic damping, which is included in the exact aerodynamic theory, eliminated the zero-dynamic-pressure flutter points. The exact aerodynamic theory also indicated changes in flutter mode similar to the changes given by the approximate aerodynamic theory. Most experimental investigations have indicated no apparent variations of flutter-mode shapes with stress, and the variations indicated by theory have been considered a discrepancy (ref. 36). Although a recent investigation (ref. 26) reported variations of position of maximum flutter amplitude with stress, additional experimental information is needed to clarify the situation.

Effects of damping.- The dashed and dot-dashed curves shown in figure 9 represent results obtained from the exact aerodynamic theory for values of the structural damping coefficient  $g$  of 0.010 and 0.025, respectively. As can be seen, structural damping has a large effect near regions where the approximate aerodynamic theory predicts zero values of the flutter dynamic pressure, but this same trend was observed for the approximate aerodynamic theory when damping was added to the analysis (ref. 36). The inclusion of damping in the analysis tends to smooth out the saw-toothed-like boundary and the resulting flutter trends might be considered to be in qualitative agreement with existing experimental boundaries.

The results of figure 9 suggest that aerodynamic and structural damping have less effect on the flutter boundaries as  $\frac{N_x}{N_{x,cr}}$  approaches 1.0. To determine the validity of this apparent trend, additional calculations were made for panels with length-width ratios of 2.45 and 1.41. These length-width ratios were chosen as they are the values for

which the approximate aerodynamic theory indicates  $\lambda^{1/3}$  to be zero for  $\frac{N_x}{N_{x,cr}} = 1.0$  for the conditions specified (all edges simply supported,  $N_y = 0$ ). These results (and the results for  $\frac{a}{b} = 4$ ) are shown in figure 10 in terms of the flutter parameter  $\lambda^{1/3}$  and the length-width-ratio midplane stress parameter  $\bar{A}$ . The solid curve is the flutter boundary obtained from the approximate aerodynamic theory (eq. (2)). The symbols represent flutter points obtained from the exact aerodynamic theory for aluminum-alloy panels at sea level for  $M = 3$  and  $g = 0.025$ . These results were obtained for  $\frac{N_x}{N_{x,cr}}$  from 0 to 0.99 for each value of  $\frac{a}{b}$ . For the conditions specified,  $\frac{a}{b} = 1.41$  and  $\frac{N_x}{N_{x,cr}} = 1.0$  correspond to  $\bar{A} = 5$ , and  $\frac{a}{b} = 2.45$  and  $\frac{N_x}{N_{x,cr}} = 1.0$  correspond to  $\bar{A} = 13$ . Comparison of the results shown in figure 10, particularly at  $\bar{A}$  of 5 and 13, indicate that the effect of damping does decrease as  $\frac{N_x}{N_{x,cr}}$  approaches 1.0. This result is attributed to the fact that small-deflection dynamic analyses indicate a zero flutter frequency at the transition point or end point of the flat-panel boundary. (See ref. 3.) Thus, before the effects of damping on panels on the verge of buckling can be investigated, it appears necessary to utilize large deflection theory and to include other effects such as initial imperfections. Analyses utilizing large-deflection theory and including the effects

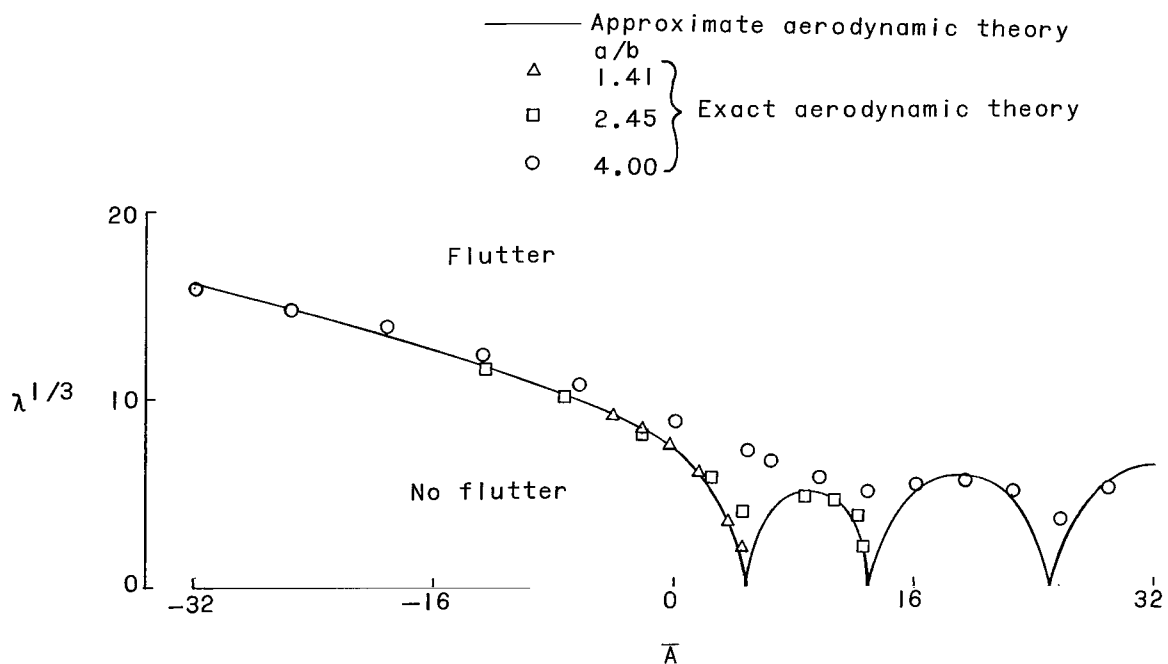


Figure 10.- Effects of structural damping on flutter of stressed simply supported aluminum-alloy panels of various length-width ratios.  $\frac{N_y}{N_x} = 0$ ;  $M = 3.0$ ;  $g = 0.025$ .

of initial imperfections (for a two-dimensional panel) are presented in references 11 and 12. However, the inclusion of damping and of a sufficient number of modes to insure convergence of the modal-type solutions for finite panels would prove extremely laborious.

The results presented in figures 9 and 10 indicate that the use of exact aerodynamic theory appears to have little effect on the differences between theory and experiment for flutter of stressed panels. Although structural damping can have a significant effect, the appropriate value of the damping coefficient  $g$  is usually not known; thus, the inclusion of structural damping to provide better flutter predictions may not be completely satisfactory. It should be pointed out that most experimental investigations of stressed panels did not include measurements or control of initial imperfections and considered differential pressure in an approximate manner, if at all. In addition, the panels were usually subjected to nonuniform temperature increases and the stress distributions are imperfectly known at best. It would appear that these factors must be considered in both theoretical and experimental flutter investigations if adequate correlations are to be obtained.

Effect of Mach number. - Calculations were made for  $\frac{a}{b} = 4$ ,  $N_y = 0$ , and  $M = 1.4$  for comparison with the  $M = 3$  results of figure 9 in order to investigate the effect of Mach number on flutter of stressed panels. Figure 11 shows the variation of the flutter parameter  $\lambda^{1/3}$  with the stress ratio  $\frac{N_x}{N_{x,cr}}$  for  $0 \leq \frac{N_x}{N_{x,cr}} \leq 0.6$ ; the structural damping coefficient  $g$  is zero.

The results for  $\frac{N_x}{N_{x,cr}} = 0$  are similar to the trends presented earlier for unstressed panels for  $\frac{a}{b} > 2.0$  in that the results for  $M = 1.4$  are slightly higher than the results for  $M = 3$ . As the stress is increased, the trend remains the same although the differences in the results for  $M = 1.4$  and  $M = 3$  become larger, particularly near  $\frac{N_x}{N_{x,cr}} = 0.575$  where there is a pronounced dip in the boundary obtained for  $M = 3$ .

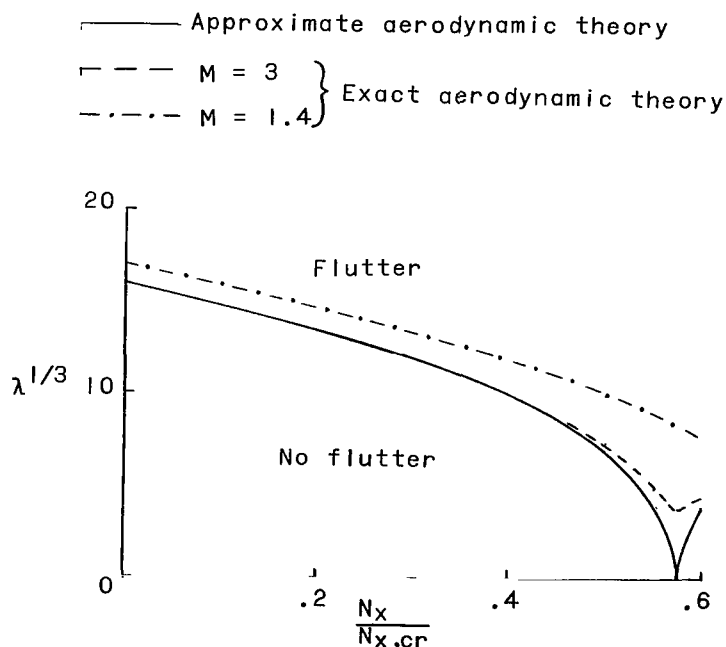


Figure 11.- Comparison of results obtained from exact aerodynamics for  $M = 3$  and  $M = 1.4$  for flat simply supported panel subjected to mid-plane compressive load.  $\frac{a}{b} = 4.0$ ;  $\frac{N_y}{N_x} = 0$ ;  $g = 0$ .

There was no other effect of variations in Mach number with increases in compressive midplane stress. The value of  $\bar{A}$  for the panel considered ( $\frac{a}{b} = 4$ ,  $N_y = 0$ , simply supported edges) and  $\frac{N_x}{N_{x,cr}} \approx 0.5$  corresponds to the value for an unstressed square panel.

The exact aerodynamic theory indicates that at  $M = 1.4$  the flutter boundary for an unstressed square panel is given by a single-degree-of-freedom instability. However, no such instabilities were found for the stressed panel.

### CONCLUDING REMARKS

Results obtained from analyses utilizing both two-dimensional static (approximate) aerodynamic and linearized three-dimensional unsteady (exact) aerodynamic theories are presented and compared. Calculations were made for both unstressed and stressed panels by using these inviscid aerodynamic theories.

The calculations for unstressed panels revealed that the results obtained from the approximate aerodynamic theory were in good agreement with the results obtained from the exact aerodynamic theory for Mach number  $M \geq 1.3$  and for panel length-width ratios  $2 \leq \frac{a}{b} \leq 6$ . For  $M \geq 1.6$  the agreement was good for  $0 \leq \frac{a}{b} \leq 6$ . For  $M < 1.6$  the exact aerodynamic theory predicted single-degree-of-freedom instabilities for  $\frac{a}{b} < 2$  that are not given by the approximate aerodynamic theory. The single-degree-of-freedom flutter boundaries usually gave much lower values of dynamic pressure required for flutter compared to the approximate aerodynamic theory.

The theoretical results were in reasonable agreement with experimental results obtained at various Mach numbers from 1.2 to 5 for  $\frac{a}{b}$  from 1 to 10. Theoretical results were also compared with experimental data obtained at various Mach numbers from 1.1 to 5 for  $\frac{a}{b}$  from 0 to 1.0. This comparison indicated that the results obtained from the approximate aerodynamic theory were in good agreement with experiment for  $M \geq 2$ , but gave unconservative predictions and were in only fair agreement for  $M < 1.6$ . However, for this range of  $M$  and  $\frac{a}{b}$  experimental results are also in poor agreement with the predictions of the exact aerodynamic theory (presented in other investigations), although the theoretical predictions are conservative. The discrepancies that exist between theoretical and experimental results for low values of  $M$  and  $\frac{a}{b}$  are attributed to several factors such as boundary-layer and transonic nonlinearities.

The application of the exact aerodynamic theory to the flutter of stressed panels did not remove the discrepancies that presently exist between the theoretical and experimental results for stressed panels. The inclusion of structural damping was found to have a large effect in some instances and tended to eliminate some of the differences

between theory and experiment. However, it was shown that on the basis of small-deflection theory damping has no effect on flutter of panels on the verge of buckling.

Langley Research Center,  
National Aeronautics and Space Administration,  
Langley Station, Hampton, Va., May 12, 1966.

## REFERENCES

1. Kordes, Eldon E.; and Noll, Richard B.: Theoretical Flutter Analysis of Flat Rectangular Panels in Uniform Coplanar Flow With Arbitrary Direction. NASA TN D-1156, 1962.
2. Easley, J. G.; and Luessen, G.: Flutter of Thin Plates Under Combined Shear and Normal Edge Forces. AIAA J., vol. 1, no. 3, March 1963, pp. 620-626.
3. Bohon, Herman L.: Flutter of Flat Rectangular Orthotropic Panels With Biaxial Loading and Arbitrary Flow Direction. NASA TN D-1949, 1963.
4. Gaspers, Peter A., Jr.; and Redd, Bass: A Theoretical Analysis of the Flutter of Orthotropic Panels Exposed to a High Supersonic Stream of Arbitrary Direction. NASA TN D-3551, 1966.
5. Dixon, Sidney C.; Griffith, George E.; and Bohon, Herman L.: Experimental Investigation at Mach Number 3.0 of the Effects of Thermal Stress and Buckling on the Flutter of Four-Bay Aluminum-Alloy Panels With Length-Width Ratios of 10. NASA TN D-921, 1961.
6. Fralich, Robert W.: Postbuckling Effects on the Flutter of Simply Supported Rectangular Panels at Supersonic Speeds. NASA TN D-1615, 1963.
7. Schaeffer, Harry G.; and Heard, Walter L., Jr.: Supersonic Flutter of a Thermally Stressed Flat Panel With Uniform Edge Loads. NASA TN D-3077, 1965.
8. Tuovila, Weimer J.; and Presnell, John G., Jr.: Supersonic Panel Flutter Test Results for Flat Fiber-Glass Sandwich Panels With Foamed Cores. NASA TN D-827, 1961.
9. Dowell, E. H.; and Voss, H. M.: Experimental and Theoretical Panel Flutter Studies in the Mach Number Range 1.0 to 5.0. ASD-TDR-63-449, U.S. Air Force, Dec. 1963.
10. Dowell, E. H.: Experimental and Theoretical Panel Flutter Studies in the Mach Number Range of 1.0 to 5.0. ASD-TDR-63-449, Suppl. 1, U.S. Air Force, Aug. 1965. (Available from DDC as AD622831.)
11. Kobayashi, Shigeo: Two-Dimensional Panel Flutter - II. Clamped Panel. Trans. Japan Soc. Aeron. Space Sci., vol. 5, no. 8, 1962, pp. 103-118.
12. Fung, Y. C.: On Two-Dimensional Panel Flutter. J. Aeron. Sci., vol. 25, no. 3, Mar. 1958, pp. 145-160.
13. Dixon, Sidney C.; and Shore, Charles P.: Effects of Differential Pressure, Thermal Stress, and Buckling on Flutter of Flat Panels With Length-Width Ratio of 2. NASA TN D-2047, 1963.

14. Erickson, Larry L.; and Anderson, Melvin S.: Supersonic Flutter of Simply Supported Isotropic Sandwich Panels. NASA TN D-3171, 1966.
15. McElman, John A.: Flutter of Curved and Flat Sandwich Panels Subjected to Supersonic Flow. NASA TN D-2192, 1964.
16. Bohon, Herman L.; and Anderson, Melvin S.: The Role of Boundary Conditions on Flutter of Orthotropic Panels. AIAA Symposium on Structural Dynamics and Aeroelasticity, Aug.-Sept. 1965, pp. 59-69.
17. Erickson, Larry L.: Supersonic Flutter of Flat Rectangular Orthotropic Panels Elastically Restrained Against Edge Rotation. NASA TN D-3500, 1966.
18. Bohon, Herman L.: Experimental Flutter Results for Corrugation-Stiffened Panels at a Mach Number of 3. NASA TN D-2293, 1964.
19. Cunningham, H. J.: Flutter Analysis of Flat Rectangular Panels Based on Three-Dimensional Supersonic Potential Flow. AIAA J., vol. 1, no. 8, Aug. 1963, pp. 1795-1801.
20. Hedgepeth, John M.: Flutter of Rectangular Simply Supported Panels at High Supersonic Speeds. J. of Aeron. Sci., vol. 24, no. 8, Aug. 1957, pp. 563-573, 586.
21. Houbolt, John C.: A Study of Several Aerothermoelastic Problems of Aircraft Structures in High-Speed Flight. Nr. 5, Mitt. Inst. Flugzeugstatik Leichtbau. Leemann (Zürich), c.1958.
22. Movchan, A. A.: On the Stability of a Panel Moving in a Gas. NASA RE 11-21-58W, 1959.
23. Bohon, Herman L.; and Dixon, Sidney C.: Some Recent Developments in Flutter of Flat Panels. J. Aircraft, vol. 1, no. 5, Sept.-Oct. 1964, pp. 280-288.
24. Dixon, Sidney C.: Experimental Investigation at Mach Number 3.0 of Effects of Thermal Stress and Buckling on Flutter Characteristics of Flat Single-Bay Panels of Length-Width Ratio 0.96. NASA TN D-1485, 1962.
25. Dixon, Sidney C.: Application of Transtability Concept to Flutter of Finite Panels and Experimental Results. NASA TN D-1948, 1963.
26. Shideler, John L.; Dixon, Sidney C.; and Shore, Charles P.: Flutter at Mach 3 of Thermally Stressed Panels and Comparison With Theory for Panels With Edge Rotational Restraint. NASA TN D-3498, 1966.
27. Guy, Lawrence D.; and Bohon, Herman L.: Flutter of Aerodynamically Heated Aluminum-Alloy and Stainless-Steel Panels With Length-Width Ratio of 10 at Mach Number of 3.0. NASA TN D-1353, 1962.

28. Bohon, Herman L.: Panel Flutter Tests on Full-Scale X-15 Lower Vertical Stabilizer at Mach Number of 3.0. NASA TN D-1385, 1962.
29. Kobett, D. R.; and Zeydel, E. F. E.: Research on Panel Flutter. NASA TN D-2227, 1963.
30. Fung, Y. C.: Some Recent Contributions to Panel Flutter Research. AIAA J., vol. 1, no. 4, Apr. 1963, pp. 898-909.
31. McClure, J. D.: Stability of Finite Chord Panels Exposed to Low Supersonic Flows With a Turbulent Boundary Layer. Paper No. 63-21, Inst. Aerospace Sci., Jan. 1963.
32. Anderson, William J.: Experiments on the Flutter of Flat and Slightly Curved Panels at Mach Number 2.81. SM 62-34 (AFOSR 2996), Graduate Aeron. Labs., California Inst. Technol., June 1962.
33. Lock, M. H.; and Fung, Y. C.: Comparative Experimental and Theoretical Studies of the Flutter of Flat Panels in a Low Supersonic Flow. AFOSR TN 670, Guggenheim Aeron. Lab., California Inst. Technol., May 1961.
34. Sylvester, Maurice A.; and Baker, John E.: Some Experimental Studies of Panel Flutter at Mach Number 1.3. NACA TN 3914, 1957. (Supersedes NACA RM L52I16.)
35. Nelson, Herbert C.; and Cunningham, Herbert J.: Theoretical Investigation of Flutter of Two-Dimensional Flat Panels With One Surface Exposed to Supersonic Potential Flow. NACA Rept. 1280, 1956. (Supersedes NACA TN 3465.)
36. Guy, Lawrence D.; and Dixon, Sidney C.: A Critical Review of Experiment and Theory for Flutter of Aerodynamically Heated Panels. Symposium on Dynamics of Manned Lifting Planetary Entry, S. M. Scala; A. C. Harrison; and M. Rodgers, eds., John Wiley and Sons, Inc., c.1963, pp. 568-595.
37. Kobayashi, Shigeo: Flutter of Simply Supported Rectangular Panels in a Supersonic Flow. Trans. Japan Soc. Aeron. Space Sci., vol. 5, no. 8, 1962, pp. 79-89.

*"The aeronautical and space activities of the United States shall be conducted so as to contribute . . . to the expansion of human knowledge of phenomena in the atmosphere and space. The Administration shall provide for the widest practicable and appropriate dissemination of information concerning its activities and the results thereof."*

—NATIONAL AERONAUTICS AND SPACE ACT OF 1958

## NASA SCIENTIFIC AND TECHNICAL PUBLICATIONS

**TECHNICAL REPORTS:** Scientific and technical information considered important, complete, and a lasting contribution to existing knowledge.

**TECHNICAL NOTES:** Information less broad in scope but nevertheless of importance as a contribution to existing knowledge.

**TECHNICAL MEMORANDUMS:** Information receiving limited distribution because of preliminary data, security classification, or other reasons.

**CONTRACTOR REPORTS:** Technical information generated in connection with a NASA contract or grant and released under NASA auspices.

**TECHNICAL TRANSLATIONS:** Information published in a foreign language considered to merit NASA distribution in English.

**TECHNICAL REPRINTS:** Information derived from NASA activities and initially published in the form of journal articles.

**SPECIAL PUBLICATIONS:** Information derived from or of value to NASA activities but not necessarily reporting the results of individual NASA-programmed scientific efforts. Publications include conference proceedings, monographs, data compilations, handbooks, sourcebooks, and special bibliographies.

*Details on the availability of these publications may be obtained from:*

SCIENTIFIC AND TECHNICAL INFORMATION DIVISION  
NATIONAL AERONAUTICS AND SPACE ADMINISTRATION  
Washington, D.C. 20546